JOURNAL OF AIRCRAFT
Vol. 48, No. 3, May–June 2011

Full-Scale Flight Tests of Active Flow Control to Reduce Tiltrotor Aircraft Download

Michael A. McVeigh*
The Boeing Company, Philadelphia, Pennsylvania 19142
Hassan Nagib†
Illinois Institute of Technology, Chicago, Illinois 60616
Tom Wood‡
Bell Helicopter Textron, Inc., Hurst, Texas 76053
and
Israel Wygnanski§
University of Arizona, Tucson, Arizona 85721

DOI: 10.2514/1.46956

The vertical force, or download, acting on the airframe of current tiltrotor configurations during hover amounts to approximately 10% of rotor thrust, or about 6000 lb for the V-22. Various mechanical means have been experimentally tried to reduce this penalty, but none has been implemented, largely because of mechanical complexity. This paper describes the research conducted on the application of active flow control to the problem, since this technique may offer a solution without large weight penalties and unacceptable complexity. The research was conducted as part of the Defense Advanced Research Projects Agency Micro Adaptive Flow Control program. The work culminated in June 2003, when the NASA/U.S. Army/Bell XV-15 tiltrotor aircraft was used to successfully demonstrate the effectiveness of active flow control in reducing airframe download during hover. The wing flaps were fitted with zero-mass-flow actuators that periodically injected/removed air in the flap upper surface boundary layer through slots from the interior of the flap. The active flow control was effective in delaying flow separation from the flap, which reduced the download on the wings. The flight tests were the culmination of extensive laboratory experiments on two-dimensional models and on a powered full-span 16%-scale model of the XV-15 aircraft. The XV-15 flight tests confirmed the laboratory findings by successfully reducing the download measured in hover by as much as 14%, demonstrating that the aerodynamic principles of active flow control can be applied to full-scale air vehicles.

Nomenclature

A	=	disc area of two rotors, m^2
c	=	wing chord, flaps up, m
C_d	=	section drag coefficient, drag$/(1/2\rho V_\infty^2 c)$
C_P	=	rotor power coefficient, 550 total rotor horsepower$/(\rho A V_T^3)$
C_T	=	rotor thrust coefficient, total thrust$/(\rho A V_T^3)$
C_W	=	aircraft weight coefficient, weight$/(\rho A V_T^2)$
C_μ	=	momentum coefficient, $2(h/x)(V_j/V_\infty)^2$
C_1	=	section lift coefficient, lift$/(1/2\rho V_\infty^2 c)$
DL	=	wing download, N
f	=	blowing frequency, Hz
F^+	=	nondimensional frequency, fx/V_∞
h	=	slot width, m
R	=	rotor radius, m
T	=	thrust of two rotors, N
v	=	rotor wake velocity, m/s, positive down toward wing
V_j	=	rms jet exit velocity, m/s
V_T	=	rotor-tip speed, m/s
V_∞	=	remote windspeed, m/s
W	=	aircraft weight, N
x	=	distance from actuation slot to trailing edge, m
α	=	angle of attack, °
δ_f	=	flap deflection, °
δ_K	=	Krueger flap deflection, °
ρ	=	air density, kg/m^3

Received 1 September 2009; revision received 6 November 2010; accepted for publication 6 November 2010.

*Senior Technical Fellow, Mail Stop P23-15, P.O. Box 16858; michael.a.mcveigh@boeing.com. Senior Member AIAA.

†Professor, MMAE Department, 10 West 32nd Street, Room 243; nagib@iit.edu. Fellow AIAA.

‡Director of Flight Technology and Simulation, Mail Stop 1343, 600 East Hurst Boulevard; twood@bellhelicopter.textron.com.

§Professor, AME Department; wygy@ame.engr.arizona.edu. Fellow AIAA.

I. Introduction

THIS paper presents a technical history of the first application of periodic active flow control (AFC) to a manned operational aircraft. It describes a number of the important milestones of this cooperative research program and focuses on some of the problems encountered and the solutions provided.

Tiltrotor aircraft (Fig. 1) experience a large download force in hover primarily caused by the rotor downwash impinging on the wings and that part of the fuselage between the wings. To minimize the download and increase net vertical lift, current design practice [1] is to deflect the flaps/ailerons to an angle of about 65° to reduce the area exposed to the rotor downwash. The resulting download is approximately 10% of the rotor thrust. However, when the flaperons are deflected to a larger angle, the flow separates in the vicinity of the flap shoulder and the download increases substantially. Various ways to decrease tiltrotor download have been explored via two-dimensional (2-D) flap tests [2,3]. Steady blowing [4] and wing-mounted mechanical devices [5] have been demonstrated to reduce the download. However, weight and complexity have prevented these solutions from being reduced to practice.

While steady blowing over the deflected flap has been shown to delay separation and reduce the vertical drag on 2-D flapped airfoils at large negative angles of attack, a more attractive technique is periodic excitation [6], which provides similar benefits but at much lower energy requirements.

Fig. 1 NASA/U.S. Army/Bell XV-15 tiltrotor in hover.

The application of periodic AFC to the tiltrotor hover download problem was suggested by J. McCroskey, of NASA Ames Research Center, during a visit to Tel-Aviv University where he had observed a demonstration of stall delay on a wing section by a pulsating zero-mass-flux jet emanating from a narrow slot. Heeding his suggestion, the validity of using the same technique to reduce vertical drag was proven by testing the airfoil at a large negative angle of attack. The result (Fig. 2) demonstrated that periodic actuation at a reduced frequency $F^+ = 1.6$ required an order-of-magnitude lower level of blowing than steady blowing for approximately the same level of drag reduction, i.e., 30%. These results provided the impetus for the initiation of an extensive AFC research program using V-22 wing section models and a powered scale model of the V-22 Osprey tiltrotor. Most of the aerodynamic tests that followed were aimed at reducing the download, and they were conducted at the University of Arizona on the V-22 model in the hover mode. Based on the test results showing that AFC was effective, a program decision was made by R. Wlezien of the Defense Advanced Research Projects Agency to conduct a full-scale demonstration of AFC on the NASA/U.S. Army/Bell XV-15 tiltrotor airplane. To prepare for this, a 16%-scale model of the XV-15 wing airfoil and a full-span 16%-scale powered model of the aircraft were built to explore AFC parameters before designing the aircraft hardware and preparing the aircraft for hover testing. This involved close cooperation with the Bell Helicopter Textron, Inc., XV-15 flight-test team. Finally, in order to gain additional insight into the phenomena observed in the tests, a large-eddy simulation (LES) computational fluid dynamics (CFD) model of the XV-15 airfoil was developed and exercised to visualize the flow patterns and relate these to the test results.

From the V-22 model download testing, model-scale AFC actuators were already available for use in the XV-15 model tests. However, small, light, robust, and reliable actuators suitable for flight were not available and had to be developed in time for the hover testing on the XV-15 aircraft. Hassan Nagib, from the Illinois Institute of Technology (IIT), was tasked with the development of these actuators to be fitted inside the flaps of the aircraft [7]. Under his leadership, the IIT team successfully developed palm-sized electromagnetic actuators for the flight demonstration. This effort is detailed in [7].

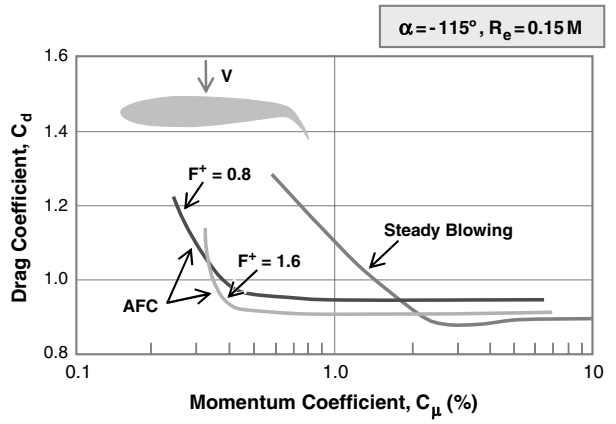

Fig. 2 Demonstration of effect of unsteady vs steady blowing on vertical drag reduction of a flapped airfoil.

II. Active Flow Control Parameters

The main parameters characterizing AFC on a surface are the amplitude and frequency of forcing, the waveform type (sinusoidal, burst mode, or amplitude modulated), the flow Reynolds number, the slot width, and a characteristic surface length downstream of the actuator. Actuators are usually placed upstream of the separated flow region.

Assuming that separated flow is independent of Reynolds number, provided it is sufficiently high, two nondimensional parameters are generally used to characterize the flow: a momentum coefficient and a reduced frequency. The momentum coefficient C_μ of a jet of width h is the ratio of the jet momentum to the momentum of the freestream. In the case of a purely sinusoidal jet flow, the jet momentum is proportional to the amplitudes of the velocity oscillations. Thus,

$$C_\mu = \left(\frac{2h}{c}\right)\left(\frac{V_{\text{jet}}(\text{RMS})}{V_\infty}\right)^2 = \left(\frac{2h}{c}\right)\left(\frac{V_{\text{jet}}\text{peak}/\sqrt{2}}{V_\infty}\right)^2 = \left(\frac{h}{c}\right)\left(\frac{V_{\text{jet}}\text{peak}}{V_\infty}\right)^2$$

The reduced frequency F^+ relates the forcing frequency to the speed of the flow:

$$F^+ = \frac{f \times x}{V_\infty}$$

This term represents the ratio of the distance over which the control of separation has to be achieved (i.e., the distance from the slot to the trailing edge of the controlled surface) to the wavelength of the dominant oscillation.

III. Model-Scale Actuators

Actuators used during the V-22 model tests and the initial XV-15 model tests were supplied by Domzalski Machine of Mesa, Arizona. In the later XV-15 model tests, Nagib et al. [7] designed an improved set of electromagnetic actuators (Fig. 3). This design used voice coils to deliver high peak jet velocities over a wide frequency range without the need for a cooling system. The square frames were designed to fit together to form a linear spanwise array beneath slots cut into the upper airfoil surface cover plates at various chordwise distances. The top surfaces of the actuator frames were sealed against

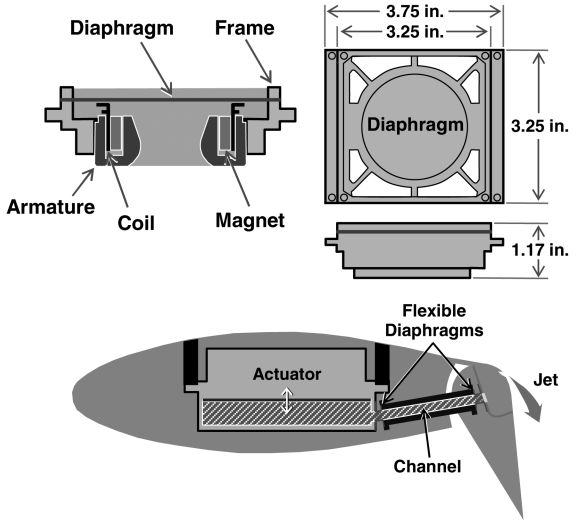

Fig. 3 Schematic of actuators.

the lower surface of the cover plate. However, for the model tests, there was not enough room in the flaps to accommodate the actuators, so they were mounted in the main element of the airfoil, and ducts were used to channel the output to slots in the flap upper surface.

Since the mechanism for delaying separation depends on the magnitude and frequency of the excitation, the model actuators provided a broad range of these parameters. The general frequency range of the coils was from 50 to 300 Hz at an input amplitude of 0 to 9 V per actuator. This in turn provided a range of C_μ from 0 to 2.5% at $0.6 < F^+ < 2.1$ and much higher values of C_μ at some specific frequencies. By varying these values together with changes in chordwise slot location and flap deflection, an optimum configuration for download reduction could be determined.

IV. Large-Eddy Simulation Flowfield Computations

To get an idea of the flow patterns and pressures to be expected in the tests, calculations were performed using LES [8] for an airfoil at an $-85°$ angle of attack with a flap deflected at 80°. Some of the calculated instantaneous pressure contours are shown in Fig. 4. During hover, the airfoil is a bluffbody for which the drag is associated with strong vortex shedding. The pressure contours, at the time when the oscillatory C_d is close to its maximum, show the presence of a large vortex close to the base of the airfoil. This vortex is created by the roll up of the mixing layer that separates the dead air in the lee of the airfoil from the rotor downwash that surrounds the wing. This mixing layer is susceptible to the Kelvin–Helmholtz (K–H) instability that creates the smaller array of vortices visible below the leading and trailing edges of the airfoil. The strength of the K–H vortices increases initially with increasing distance from the separation location before dissipation sets in and weakens them. The instability of the vortex array generates a large circulation pattern that rotates in the counterclockwise direction in the mixing layer created near the leading edge of the airfoil. Near the trailing edge, the circulation is in the clockwise direction.

These circulation patterns affect the instantaneous pressure distribution around the airfoil and cause an oscillation in the stagnation location on the upper surface that results in periodic vortex shedding. When the K–H eddies are created naturally, due to random disturbances in the flow, they vary in strength and are more susceptible to early roll up near the base of the airfoil. This generates low pressure on the bottom surface of the airfoil and results in large drag oscillations. The contours shown in Fig. 4b correspond to an instantaneous minimum in C_d, because the large circulation pattern (Fig. 4a) has been swept downstream, and only some shear layer (K–H) vortices are present close to the base of the airfoil. In Fig. 4c, eddies created by controlled periodic excitation (AFC) at a point near the flap shoulder are more regular and resistant to the secondary instability and large roll up. The pressure contours of Fig. 4c suggest that a weak circulation pattern might have been created one chord length below the airfoil. Such a pattern has only a minor effect on the pressure distribution over the airfoil and will substantially reduce the oscillations in drag. Two additional observations may be made by comparing flow patterns in Figs. 4a and 4b with Fig. 4c:

1) The periodically excited flow stays attached to the flap instead of separating from it.

2) Periodic excitation applied to the trailing-edge flap effectively regulates the shedding of vortices created in the mixing layer formed near the leading edge of the airfoil. Thus, application of additional excitation near the wing leading edge must be coordinated with the phase of the excitation on the flap in order to be effective.

V. Wind-Tunnel Tests

Tests were made on 2-D models of a flapped XV-15 airfoil in which various means to reduce vertical drag were evaluated. The more promising approaches were then tested in a hover download test rig using the powered model of the XV-15.

A. Two-Dimensional Airfoil Vertical Drag Tests: Test Setup

Experiments [9,10] were conducted on a 2-D 10.08 in. chord (16% scale) flapped XV-15 wing airfoil model in University of Arizona's 24 by 41 in. wind tunnel. Part of each sidewall was removed to avoid large blockage corrections (Fig. 5). The sidewalls terminated upstream of the airfoil at the scaled height of the rotor above the wing of the airplane. The sidewall opening allowed the flow to go around the wing section as if in free air.

The XV-15 wing airfoil (NACA 64A223 mod) spanned the 24 in. height of the tunnel. It was machined from aluminum and provided with a chordwise row of pressure taps at the center span. Five 0.04-in.-wide inline spanwise slots were machined into the flap upper surface for fluidic actuation. Each slot was spaced apart by a short distance from its neighbor to preserve the structural integrity of the surface. The interruption of the slots caused only a small local reduction in the momentum of the jets.

The 25% chord plain flap was hollow to accommodate AFC actuation ducting. The interior of the main airfoil, also hollow, served as a settling chamber for actuation from outside the tunnel or accommodated a spanwise array of internal actuators.

The ducts from the actuators to the slots and all their connections were identical. The actuators were all manufactured with identical impedance and were designed to have the same performance so as to give as much spanwise uniformity as possible. The slots delivered the air at an angle of approximately 30° to the flap upper surface, which was determined to be optimal based on prior testing. The amplitudes of the jet oscillations from each slot were measured, and the actuators were matched so that their sensitivity to input voltage did not vary by more than $\pm 5\%$ from slot to slot. The sensitivity to frequency variation was greater, amounting to $\pm 10\%$ for frequencies of 160 Hz and higher. This variance was halved at forcing frequencies that were

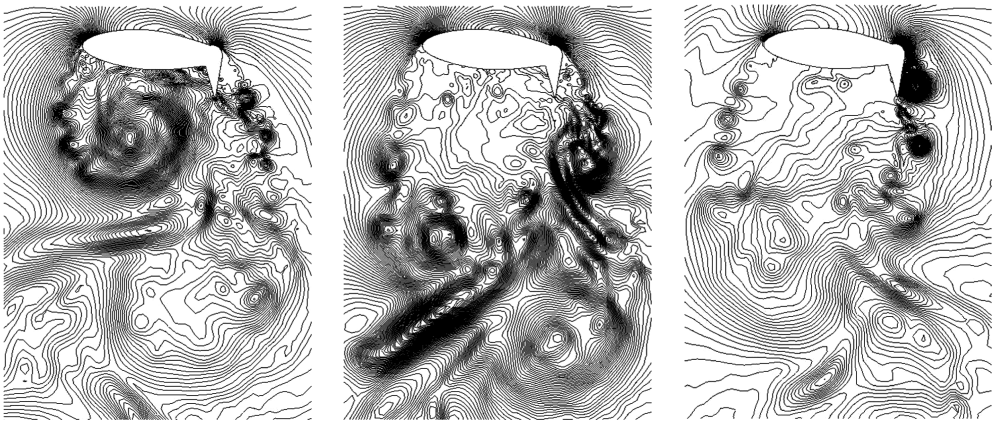

a) Baseline at maximum computed c_d

b) Baseline at minimum computed c_d

c) Periodic excitation applied from a slot at 10% flap chord

Fig. 4 Computed instantaneous pressure contours showing characteristic structures in flowfield.

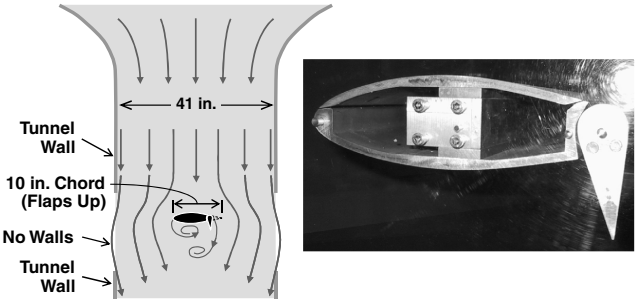

Fig. 5 2-D airfoil in partially open wind-tunnel test section.

below 100 Hz. Following a few tests, the flow through the slots was checked again to make sure that there was no degradation in actuator performance.

B. Test Results Without Krueger Flap

The 2-D tests explored the effect of actuator-slot position, amplitude of the periodic excitation C_μ, its frequency F^+, flap deflection angle, and the airfoil angle of attack with respect to the tunnel velocity, representing the rotor downwash velocity.

Based on data from wake surveys, the vertical drag on the wing sections was about 95% pressure drag, so the measured pressure drag was taken as representative of the total vertical drag. The normalized drag and lift coefficients on the 2-D model (Fig. 6) were obtained at a representative $\alpha = -85°$. The Reynolds number was 250,000, and the slot was located at 10% flap chord, which was upstream of the observed flow separation point. The download without actuation (the slot was taped over) decreased with increasing δ_f, reaching a minimum value of 0.72 at 55°, and then it increased at higher angles

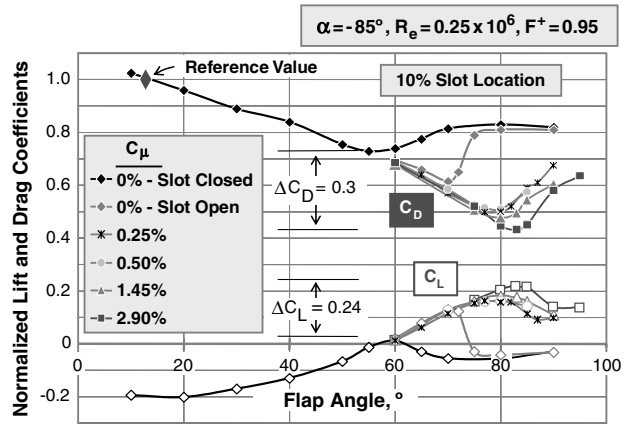

Fig. 6 2-D airfoil section drag and lift, with and without AFC.

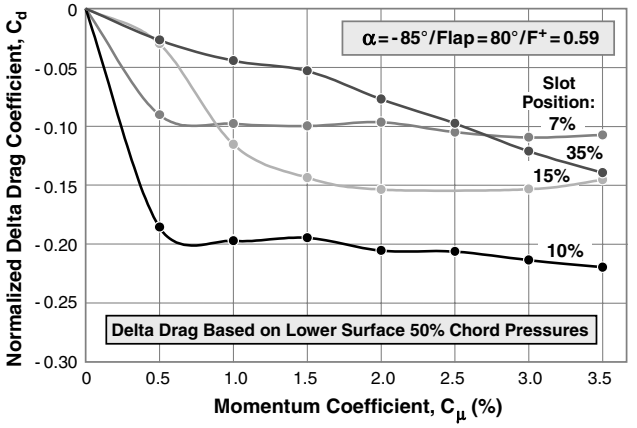

Fig. 7 Effects of slot location and C_μ on the download of the 2-D section.

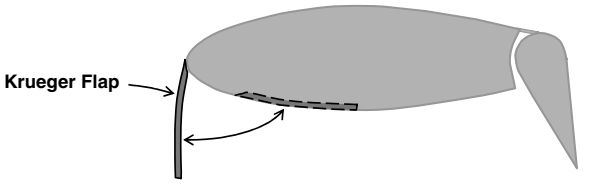

Fig. 8 XV-15 airfoil with Krueger flap.

due to increasing separation to a constant $C_d \approx 0.83$ at $\delta_f > 70°$. When the slot was opened (but with no AFC applied), internal cavity resonance, which included the sealed ducting, further reduced the C_d to 0.61 by maintaining attached flow on the flap up to $\delta_f = 70°$.

When AFC was applied at a reduced frequency of $F^+ = 0.95$, and the minimum C_d was moved to $\delta_f \approx 80°$, depending on the value of C_μ. The largest reduction was with $C_\mu = 2.9\%$, which reduced the relative drag by $\Delta C_d = 0.3$ (41%) compared with the minimum without AFC. Lowered section drag was accompanied by an increase in the orthogonal lift force (lower part of Fig. 6), which is a chordwise force toward the rear of the aircraft sometimes referred to as suckback. This increased from about zero at $55° < \delta_f < 60°$ to a normalized $C_l = 0.22$ at $\delta_f = 80°$. On the tiltrotor aircraft, this force would be canceled by a small amount of forward nacelle tilt.

Determination of the optimal slot location, and the best values of C_μ and F^+, would have required many measurements of the chordwise pressures distributions. To avoid this, the drag was derived from the C_p measured at a single pressure tap located at midchord on the lower surface of the airfoil. Since the pressure over the airfoil's lower surface was constant and the maximum C_p over the upper surface was unity (stagnation), the ΔC_p was used to determine the drag accurately and consistently following a short calibration process.

The effect of C_μ on the section drag is presented in Fig. 7 for various locations of the slot at a constant value of $F^+ = 0.59$. Note the large reduction in drag at small values of C_μ that occurred with the slot positioned at 7 and 10% chord and the subsequent insensitivity of C_d to further increases in C_μ. For the more rearward slot positions of 15 and 35%, however, increasing C_μ above 0.5% continued to reduce the drag significantly but not below the levels attained with the slot at 10% chord.

C. Test Results with Krueger Flap

A Krueger flap (Fig. 8) was attached to the leading edge of the 2-D airfoil and evaluated for its effect on reducing the download [11]. The length of the Krueger was approximately 25% of the chord and was shaped to conform to the front portion of the lower surface of the airfoil rearward of 10% chord. Figure 9 presents the variation of C_d with flap deflection for three Krueger settings of 90, 100, and 110°, with and without AFC applied to the flap or to the Krueger.

The passive Krueger (i.e., no AFC applied), when deflected at 90° to the chord, showed a small reduction in drag with the minimum occurring at 63° flap deflection. When strong AFC ($C_\mu = 3.4\%$) was

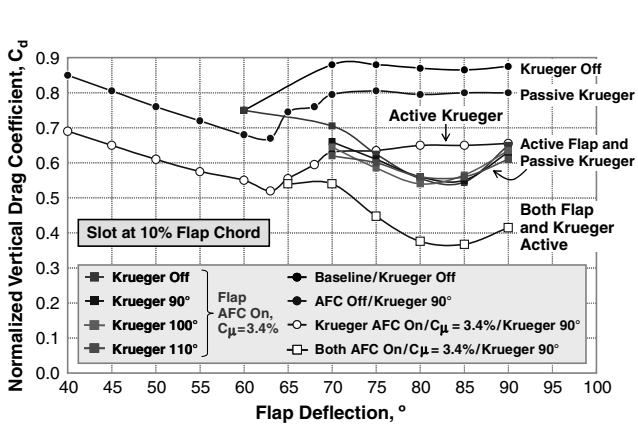

Fig. 9 Effect of Krueger flap on vertical drag of XV-15 airfoil section.

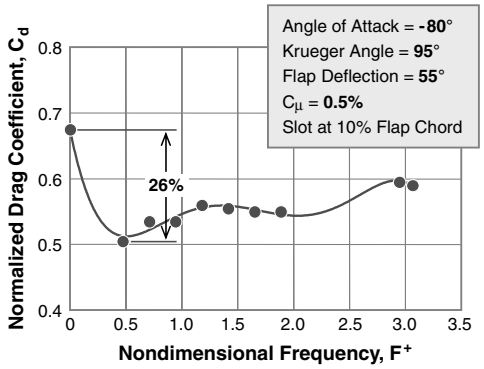

Fig. 10 Variation of C_d with actuation frequency F^+.

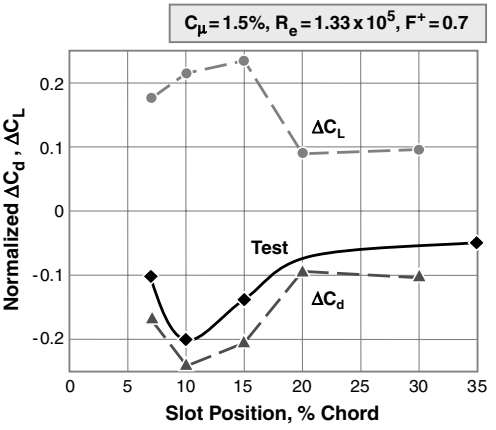

Fig. 11 LES-computed variation of ΔC_l and ΔC_d with slot location.

applied to only the Krueger near the leading edge, a drag reduction of almost 30% occurred compared with the baseline with no Krueger and AFC off. With AFC applied to the flap but not to the Krueger, minimum drag occurred at a flap setting of 83°, regardless of Krueger angle. When both the flap and the Krueger had AFC applied to them, a reduction in minimum drag of about 50% was achieved. Active control over the Krueger flap and no control over the trailing-edge flap provided approximately the same download alleviation as active control over the flap, with or without the Krueger; that is, when AFC was applied to the flap and the Krueger was passive, there was no benefit to adding the Krueger.

The effect of actuation frequency on the drag reduction with $C_\mu = 0.5\%$ is shown in Fig. 10. For this Krueger configuration, the minimum drag occurred in the neighborhood of $F^+ = 0.5$.

The location of the oscillatory jet plays a large role in the efficiency of AFC. In Fig. 11, values for download reduction and suckback force as a function of slot position are shown. These values were obtained using the LES analysis, and they compare favorably with the experimental data. Note that the LES predicted the optimal slot location to be around 10% flap chord.

The time-averaged pressure distributions over the airfoil and flap for the unforced and forced cases are shown in Fig. 12, where the experimental results are indicated by interconnected symbols, and the results obtained by the LES are represented by smooth curves. There is good agreement between the LES and the experimental results, validating the calculation technique. The impingement of the flow on the upper surface results in a positive Cp over the main element. Stagnation pressure ($Cp \approx 1$) occurs near the midchord of the main element. The flow then accelerates toward the leading edge and toward the flap. The flow separates at the main airfoil leading edge and at the upper surface of the flap shoulder due to the large flap angle.

The negative base pressure on the lower surface of the airfoil is almost constant ($C_p < 0$), and it is approximately the same over the separated region of the flap upper surface. AFC applied to the flap upper surface increases the base pressure on the airfoil lower surface and substantially lowers the pressure over the upper surface of the flap by attaching the flow over the shoulder. Both effects reduce the download.

The Krueger flap effects predicted by the LES computations (Fig. 13) showed relatively little effect when the flow separated from both flaps, but they showed a large effect when periodic excitation reattached the flow. When the wavelength of the excitation was commensurate with the length of the flap, the calculated C_d was 0.4, while the measured value was 0.38. The computed pressure contours again indicate that forcing the flow at a suitable frequency regulates and equalizes the K–H eddies that are formed in the mixing layer, making them more resistant to roll up into a large recirculating eddy below the airfoil. Coupled with flow reattachment over both flaps, this results in the observed drag reduction.

VI. Powered XV-15 Model Tests

A. Test Rig

The powered XV-15 model download experiments were conducted in the Aerodynamics Laboratory at the University of Arizona. The laboratory was climate controlled, with bare concrete floors and walls and a high ceiling. The XV-15 tiltrotor model was inverted and suspended from an A-frame structure, directing the rotor downwash up toward the ceiling, which was located more than five rotor diameters away (Figs. 14 and 15). This arrangement minimized the effects of the ground in the hovering condition, and the A-frame structure provided minimal interference to the flow in the vicinity of the wing. The motor and drive system was placed on the floor, with

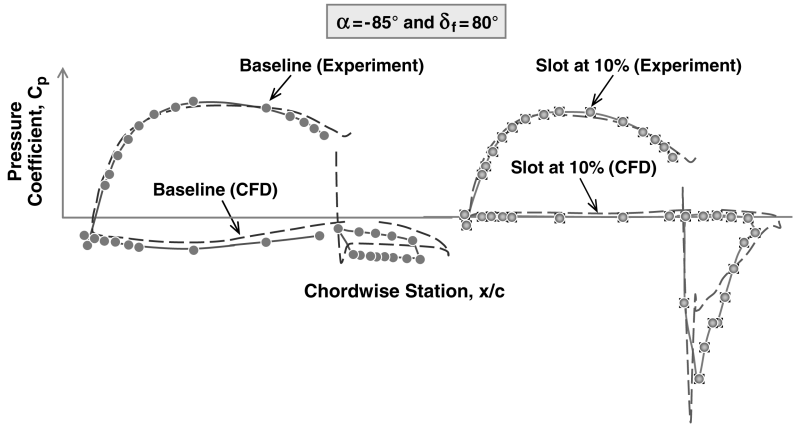

a) No excitation **b) Periodic excitation from slot at 10% flap chord**

Fig. 12 Calculated and measured *Cp* distribution.

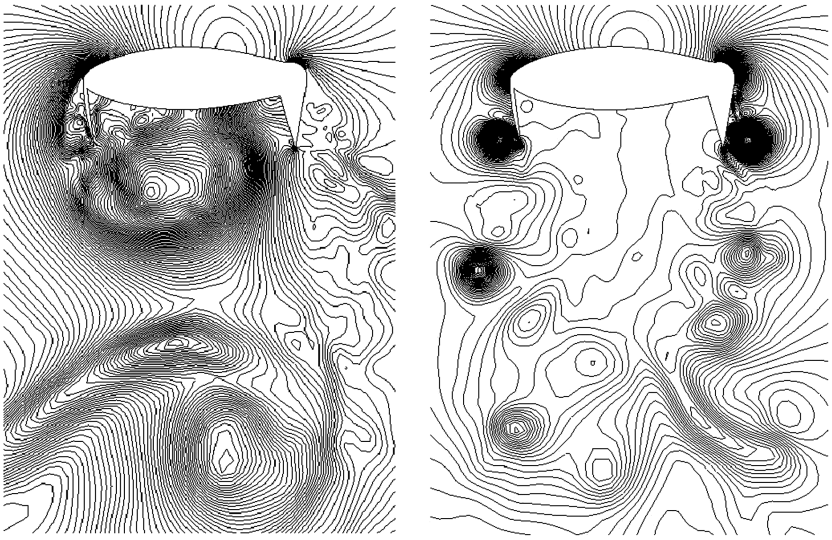

a) No excitation b) Excitation from the shoulders of both flaps

Fig. 13 Computed pressure contours for XV-15 airfoil with Krueger flap.

gearing providing the rotational motion up through two stacks to each rotor. The rotors were not connected to the nacelles to allow for a direct measurement of the aerodynamic forces on the model. The gap between the rotors and the nacelles was less than 2 in., or 4.2% of the 4-ft-diam rotors.

The bottom of the fuselage was 18 in. below the crossbar. The model consisted of a fuselage, tails, wings, adjustable ailerons and flaps, nacelles, and rotors. The bottom surface of the fuselage had hard points to attach a 0.5 in. aluminum plate. A tripod fixture suspended from the A-frame was attached to the aluminum plate by

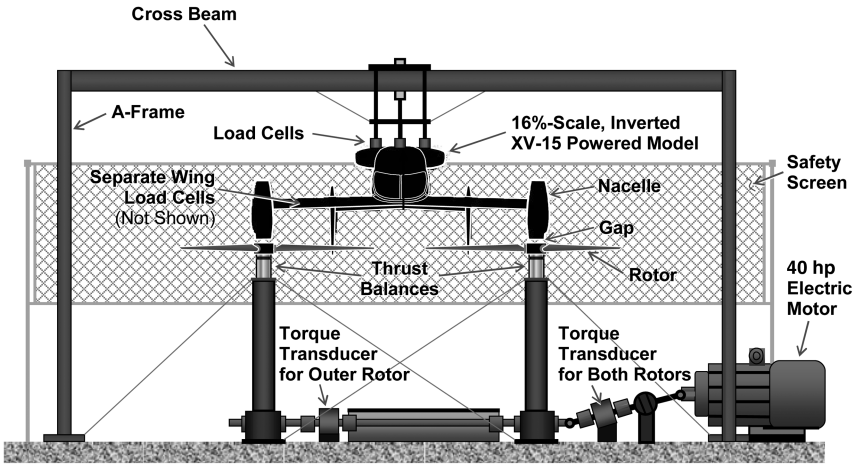

Fig. 14 XV-15 model download rig.

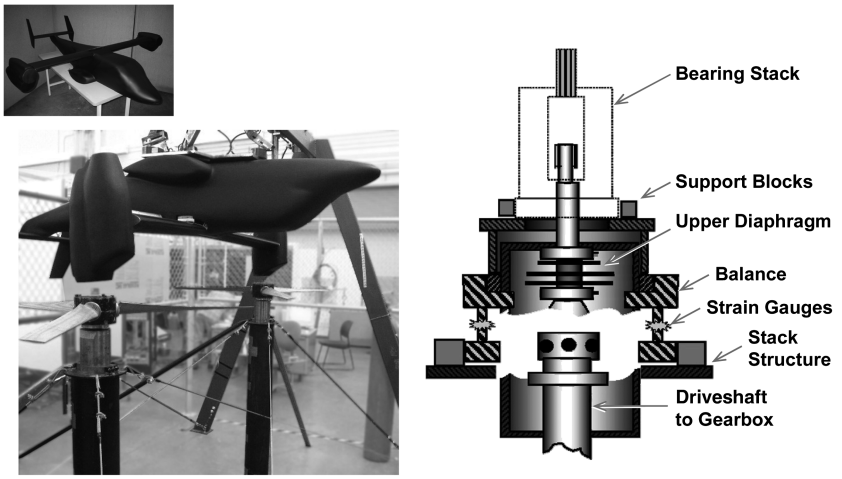

Fig. 15 XV-15 model and thrust balance schematic.

three load cells that directly measured the total aerodynamic download force. The load cells were arranged in a T-shaped configuration to provide the vertical load, rolling moment, and pitching moment.

The rotors were 4-ft-diam wooden replicas of the 25-ft-diam XV-15 rotor blades incorporating the same twist, planform, and airfoils. Each set of three blades was set in a clamshell hub that connected to a vertical driveshaft. Blade collective pitch was set by hand. A balance mounted on each rotor stack measured rotor thrust. Transducers installed at the base of each stack, inline with the horizontal drive shaft, measured rotor torque. This allowed the port transducer to measure the port rotor torque and the starboard transducer to measure the torque of both rotors. Subtraction yielded the torque of the starboard rotor. A 40 hp variable-frequency electric motor drove both rotors through a linking horizontal cross shaft. The maximum allowable continuous operating speed of the wooden blades was 2400 rpm, giving a rotor-tip speed of 500 fps.

AFC was provided by a set of five voice-coil actuators mounted inside each wing. The flexible diaphragms and ducts mated each actuator to its designated slot. The actuators generated an oscillating jet at each slot on the flap surface via flexible ducts from the wing to the inside of the flap and then to the wing slots. Three slots were located on each aileron, and two were along each inboard flap. The jets from the slots were angled at approximately 30° to the airfoil surface, a value determined to be effective from past experiments. Note that the flaps and the ailerons were deflected at the same angle in all these tests. A slot was also provided in the wing leading edge, and the output from the rear faces of the actuators was ducted to this slot in the same way, as the ducts from the front faces led to the flaps. This enabled periodic blowing and suction over a Krueger flap that could be attached to the leading edge below the slot. A Krueger flap is not a part of the XV-15 configuration, but it was planned to be evaluated in flight if the powered-model experiments indicated merit, although the 2-D test with a passive Krueger with an active flap did not yield positive results (Fig. 9).

The test procedure accounted for balance drift caused by temperature changes during a data run. The model was first warmed up at the desired rpm for about 60 s to allow the flow and the balance readings to stabilize. Data was acquired for 40 s, and then the motors were shut down. When the rotors came to a stop, a windoff data point was recorded to see if the load cells had drifted during the run. The variance in the download force measurements for 20 repeated data points for each of the three flap deflections selected was approximately 1.5%.

B. Test Results

The applicability of the 2-D results to the three-dimensional (3-D) powered model was of concern at the outset. To determine the extent to which the flow over the wing sections was 2-D, surface flow visualization was employed using tufts and surface oil flow (china clay). The wing leading-edge separation patterns created by the rotor wake are shown in Fig. 16a, which indicated that the separation from the wing leading edge was uniform along the span.

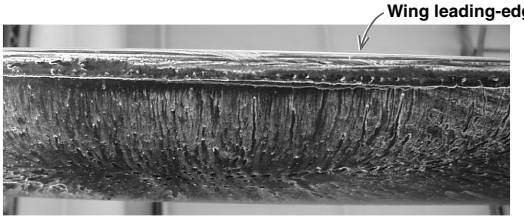

a) Separation from the leading edge

b) Separation from the flap; the nacelle is on the right- hand side of each picture

Fig. 16 Flow visualization on right-hand wing of powered model.

Separation from the deflected trailing-edge flap (it had a seal between the main element and the flap surface) appeared to be 2-D, except just inboard of the engine nacelles (Fig. 16b) where the flow separates at much smaller flap deflections. It is not clear if separation propagated evenly from the trailing edge when the flap angle was increased or if it did so along the span from the tip to the root of the wing, because a very small increase in flap deflection resulted in totally separated flow over the flap. The relative two-dimensionality of the separation line over the wing suggests that the 2-D airfoil results were representative.

To judge the effectiveness of AFC, a set of measurements without AFC were taken with the rotor wake impinging on the wing at an angle of attack of −88° for which aircraft flight-test data were available. The wing airfoil was clean and had actuation slots sealed by a thin tape pulled tightly to maintain the surface geometry. Moving the slot to different positions did not affect the measurements when the tape was in place. With the tape removed, it was noticed that the slot would introduce the effect seen in the 2-D tests; that is, an open slot leading to a closed cavity could cause cavity resonance and passively control the separation. However, comparing the taped and open slot cases showed only slight differences that did not exceed the scatter in the data.

In the 2-D tests, the addition of the Krueger flap at the leading edge was shown to reduce the download without AFC. This also occurred in the 3-D tests (Fig. 17), where the flow on the Krueger stayed fully attached, as observed with tufts, providing download reduction up to $\delta_K = 110°$. Beyond 110°, the Krueger had increasing amounts of separation that reduced its effectiveness. At a flap setting of 60°, separation was most sensitive to the Krueger deflection angle,

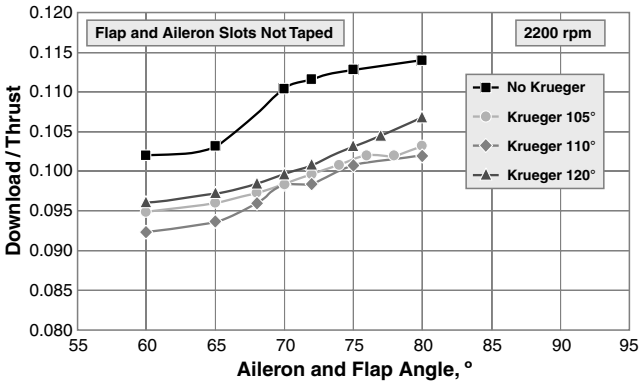

Fig. 17 Effect of Krueger on download of powered XV-15 model with no AFC.

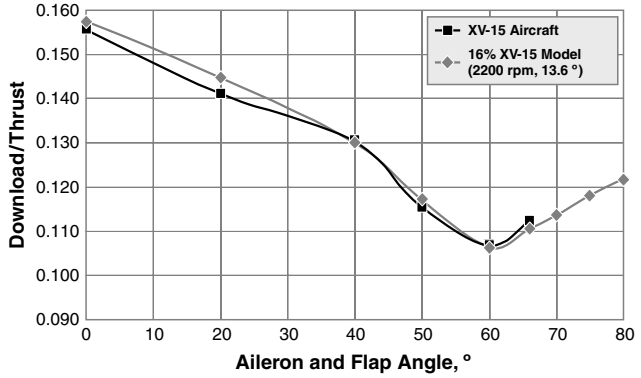

Fig. 18 Comparison of baseline download between 16% powered-model and full-scale aircraft.

because this is the flap deflection that pulls the stagnation point farthest from the leading edge. The Krueger was also sensitive to the smoothness of the transition region between the airfoil and the Krueger leading edge. Without AFC, the Krueger alone provided a download reduction of about 10% for the 3-D case, although it was less effective for the 2-D case (compare the minimum download shown in Figs. 6 and 9. However, the 2-D experiments showed that the Krueger maintained attachment up to about $\delta_k = 63°$ (Fig. 9), while in the 3-D case, it had no effect on the flap deflection at which the flow separated. The discrepancy in separation angles is attributed to the swirl angle and unsteady flow caused by the rotor in contrast with the uniform 2-D flow from the wind tunnel.

Also interesting to note in Fig. 17 is the difference in slope of DL/T vs flap deflection, with and without the Krueger. Without the Krueger, the slope is much higher from $\delta_f = 65$ to 70°, after which it becomes flatter as the flap fully separates. The presence of the Krueger may have had the effect of shifting the stagnation point more toward the leading edge and changing the pressure distribution over the flap. This effect was best seen as the flap entered incipient separation. The attached Krueger developed a forward force that opposed the attached flap suckback force, effectively canceling it. This may be important when AFC is applied to the flap, since it increases negative pressure on the flap surface, resulting in a substantial rearward force.

C. Comparison of Model Results with Full-Scale Aircraft Data

Download data obtained on the 16% XV-15 model and flight-test data from the XV-15 airplane are compared in Fig. 18. The flight-test value of download was deduced from measurements of rotor torque and aircraft weight using an estimate of installed rotor figure of merit. With C_T matched, the model data agreed with the flight results. This indicates that a scale model can realistically simulate flight conditions in hover. Therefore, it is assumed that AFC results at model scale should give reasonably accurate predictions of what AFC would give in full scale also.

D. Results with Active Flow Control Applied

The first AFC tests that were conducted used AFC on the flap only (Fig. 19). The intention was to confirm that AFC would work in 3-D, as it was shown to work in 2-D and to map out its effectiveness. The angle between the rotor thrust axis and the wing chord was set to −88°. At 2200 rpm and $C_T = 0.016$, baseline DL/T was 10.6% at 60° flap deflection [9]. With AFC turned on at $C_\mu = 3.2\%$, the download was reduced by 13%. Further reducing C_μ to 1.25% only reduced the download alleviation to 12%.

E. Effect of Passive Krueger Flap

The results in Fig. 17 showed that the Krueger with naturally attached flow would provide a benefit without AFC. However, 2-D studies indicated that with AFC on the flap, there was no observable benefit from the passive Krueger, despite its considerable value for the baseline (Fig. 9). This might be explained by the shift in the stagnation location on the airfoil upper surface due to the high negative pressure on the activated flap. This, in turn, would affect the flow over the leading edge, perhaps separating the flow over the Krueger. Therefore, the first tests conducted on the powered model with the Krueger had AFC applied to the flap only, with the Krueger set to an angle δ_K where the flow was attached as seen from the 2-D baseline data.

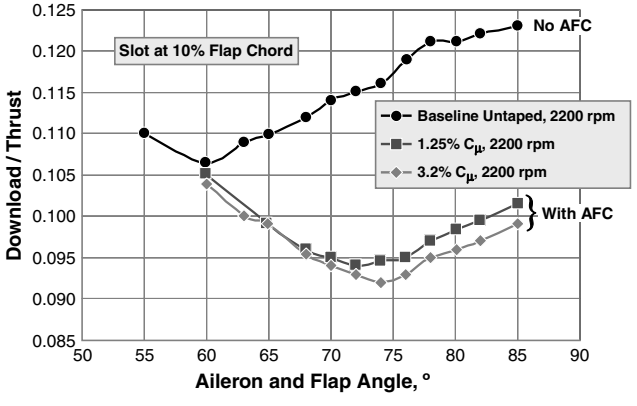

Fig. 19 Download on XV-15 16% powered model with AFC.

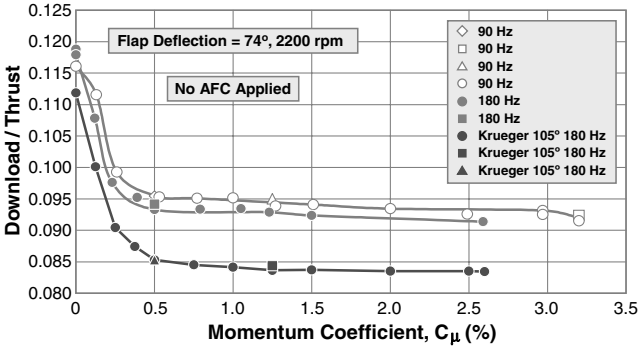

Fig. 20 Effect of $C\mu$ on XV-15 model download/thrust with passive Krueger.

The results were not the same as in the 2-D case. The passive Krueger with AFC on the flap performed better than with no Krueger for the same level of AFC, provided that the Krueger angle δ_K was properly set. In this case, the most beneficial setting was 105°. The unexpected passive Krueger benefit with an activated flap indicates that a Krueger flap could be beneficial in reducing download on a tiltrotor aircraft if employed either without the complexity of leading-edge actuation or used with leading-edge actuation but no flap AFC. To examine this further, a C_μ sweep at various δ_K was made. The results indicated that the value of a passive Krueger flap was not reduced by the application of AFC over the trailing-edge flap, even as the C_μ from the flap slot was increased. Figure 20 shows data with $\delta_k = 105°$ and $\delta_f = 74°$. Note that a threshold value of $C_\mu = 0.5\%$ was necessary to achieve most of the benefits from flap-mounted AFC. Additional increases in C_μ gave only marginal benefits.

When comparing these data to the minimum DL/T of 0.107, obtained on the basic model without a Krueger flap or AFC, AFC alone was responsible for a 16% reduction in download. In conjunction with a passive Krueger flap, the benefit increased to 23%. Figure 21 shows that, even with the passive Krueger set to $\delta_K = 120°$, where the flow over the Krueger was separated, some improvement beyond an activated flap alone was evident.

F. Effect of Active Krueger Flap

The benefits achieved on the airplane model with a passive Krueger and an active flap, which were not seen in the 2-D tests, were sufficiently encouraging to test with AFC applied to the Krueger flap. The actuator setup was such that one actuator powered both the flap

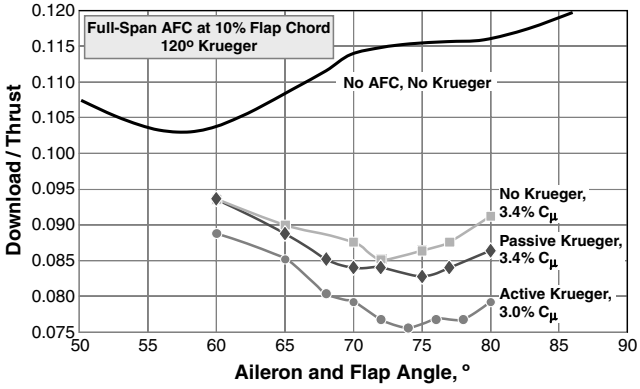

Fig. 21 Effect of simultaneous actuation on trailing-edge flap and Krueger.

slot and the leading-edge Krueger slot on the model. This was done by exposing the bottom sides of the actuator diaphragms to the Krueger slot while their top sides were connected to the trailing-edge flap. Consequently, on an actuator upstroke, compressed air would be ejected from the flap slot and sucked in through the Krueger slot. The Krueger was then inherently out of phase with the flap slot for all the tests, which were also confined to a single frequency of excitation. Since the flow over the Krueger flap was naturally attached up to $\delta_K \approx 110°$, the Krueger flap was deflected to a passive separated condition with $\delta_K = 120°$. The resulting full-span periodic actuation over both Krueger and flap yielded a download reduction of 27% (Fig. 21).

VII. XV-15 Flight Tests

A. Full-Scale Actuator Development and Integration

Nagib and his team at IIT led the full-scale actuator development and this effort resulted in a compact and reliable actuator that met the flightworthiness requirements [7]. The actuators developed for the XV-15 flight tests were larger and more powerful versions of the same basic design as the model-scale actuators. Four goals drove the design. First, the actuators were to be placed as close to the slot exit as possible to minimize losses. Second, the actuator width was sized so that the actuator arrays would cover as much of the flap span as possible. Third, the actuator depth was made as large as possible without interfering with the structural or the functional components inside the flap leading edge. Fourth, the actuators were designed and mounted so that they could be easily and quickly replaced in the event of a failure.

For the flight tests, each actuator was fitted into the flap and placed against a nose block that contained a specially shaped conduit from the actuator to the slot on the flap surface. The conduit accelerated the flow to the slot in the blowing phase, and during the suction phase, the shape of the conduit was such that flow separation within it was avoided.

With the dimensions of the actuator defined, the internal actuator components, the coil, magnet, armature, and piston were optimized to give the required forcing amplitude of 60 to 100 m/s peak velocity at the slot exit over the desired frequency range 50–100 Hz. A number of factors were considered in the material selection and component design. These factors include the significantly higher forcing amplitude that was required compared with the model, the lower frequency range, and the more hostile operating environment. A larger coil was used, along with a larger, stronger magnet and armature. The piston was designed to allow longer coil travel. New high-temperature adhesives were used. As with the actuators in the model, extensive finite element modelling was used to optimize the design of the magnet, armature, and actuator frame.

A risk-reduction task was designed to ensure smooth integration of the actuators into the aircraft and to verify actuator performance and durability under simulated flight conditions. The task involved construction of a full-scale model of a 2-D section of the XV-15 flap with actuators and AFC slot, and testing of the model in the National Diagnostic Facility (NDF) wind tunnel at IIT at the expected flight conditions.

The full-scale flap section model (Fig. 22) was designed to hold up to five actuators. The model was installed in the NDF test section with a truncated main wing element that was designed to give separated flow conditions beneath the flap and main wing similar to those seen in the powered-model tests. This would produce representative pressure differences across the actuator's diaphragm. The flap and main element were instrumented with pressure taps. The AFC slot location and design used on the flap model were identical to the location and design to be used on the aircraft that was based on the 16% model test results. The interior of the flap model was designed to closely simulate the interior of the aircraft flaps. The wiring and connectors used in the flap model were identical to those used on the aircraft. This arrangement allowed troubleshooting of any problems (such as overheating) under simulated flight conditions.

The pseudoflap test was also used to optimize the performance of the actuator arrays and to estimate their power requirements. Pressure

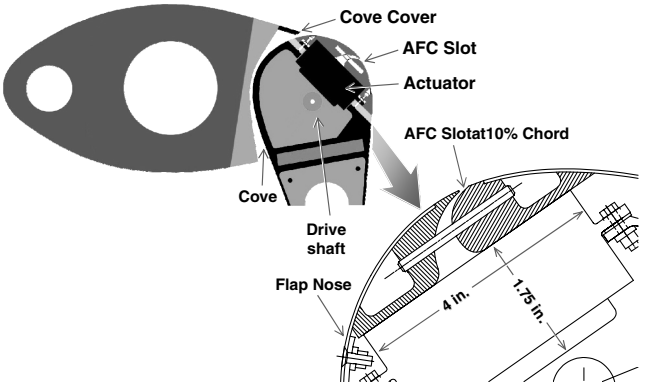

Fig. 22 Full-scale pseudoflap and the design of the slot on the aircraft.

measurements were made on the surface of the model, allowing determination of the frequency ranges and forcing amplitudes that were expected to have the greatest effect on the separation. The operating environment inside the actual XV-15 flaps was simulated and the thermal operating limits of the actuators were determined. The pressure difference across the actuator pistons was measured under these conditions and the actuator operating limits (maximum amplitude for each frequency) established for different pressure differentials.

Two commercially available audio amplifiers were used to supply power to the actuators on the aircraft. One amplifier was used to drive the set of 26 actuators on each wing. The amplifiers used a high-efficiency power supply and were internally modified to give the required output power (approximately 100 W per actuator, i.e., 2600 W per side) without overloading the power inverters on the aircraft. A wiring study was performed to determine the optimal wiring arrangement for the actuators. Detailed impedance measurements were made on individual actuators as well as groups of different numbers of actuators. Impedance was measured over a range of frequencies and operating amplitudes. The chosen wiring configuration gave the optimum distribution of available power across the span of the wing.

The actuators were installed in the flaps of the XV-15 before installing the flaps on the aircraft, Fig. 23.

A detailed series of benchtop calibrations were performed to confirm the performance of the actuators, to document the total impedance, and to test the wiring configuration. The actuators were installed in bays, 2 in.each flap and 4 in.each aileron. Following installation their output was calibrated in situ using a hot wire, Fig. 23. A special AFC controller was developed for the aircraft and was mounted in the instrument panel. Several calibrations documented the performance of the actuators for different settings of the AFC controller. They also documented the spanwise variation in forcing amplitude, the effects of leakage around the actuator frames, and the effects of varying the venting of the flap interior. These tests also allowed the operating parameters of the actuators for the flight tests to be finalized and the actuator health monitoring

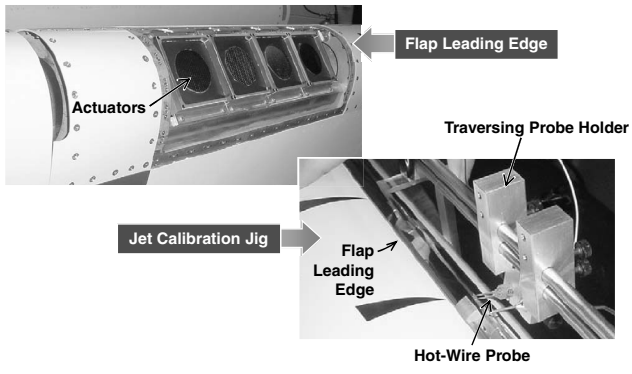

Fig. 23 Actuator arrangement and slot calibration jig for the XV-15.

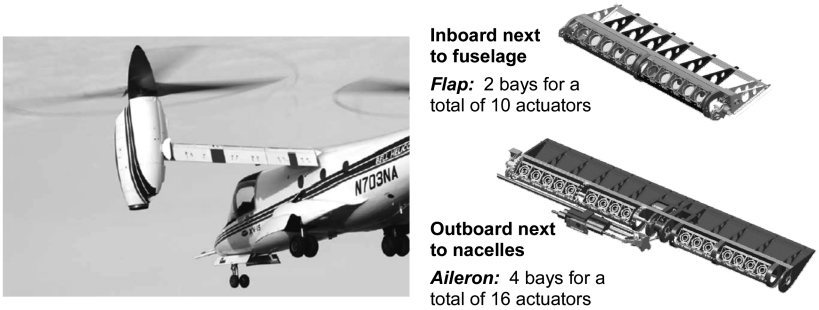

Fig. 24 Bell XV-15 during AFC test flights and the arrangement of actuators.

systems to be tested. Health monitoring included thermocouple measurements of actuator temperature and dynamic pressure measurements inside the actuator bays in the flaps.

B. XV-15 Flight-Test Results

The testing took place at Bell's Arlington, Texas, flight-test facility. The XV-15 aircraft was fitted with special-purpose flaps and ailerons, built by Bell for the test, Fig. 24. The flaps contained the actuators built by Nagib et al. [7], and the airplane was qualified for hover and very low-speed forward flight only, because the normally independent ailerons and flaps were connected to simulate the arrangement on the V-22. Each wing contained 26 actuators: 10 on the flap and 16 on the aileron. These were supplied with power via wires through the flaps connected to power-conditioning amplifiers driven by the aircraft electrical generators in the fuselage. The actuators fed air to the slots positioned at 10% chord. The width of the slots was nominally 0.045 in. A control panel in the cockpit enabled the pilot to select the frequency and overall blowing output strength of all of the actuators.

The performance goals, which were established before the flight tests, are illustrated in Fig. 25, using data from the powered-model testing. They were 1) to demonstrate that AFC could be used to reattach fully separated flow on the flap and 2) to produce a useful reduction in the minimum download by maintaining attached flow on the flap to higher flap angles that was hitherto possible. A reduction of 14% or 220 lb was targeted for goal 1, and 9% or 150 lb was targeted for goal 2. The aircraft was weighed with full fuel, and the weight of the pilots and their baggage was also determined before each flight. A fuel flow totalizer gave the amount of fuel consumed, and hence the weight at any time. Testing was conducted early in the morning when the winds were less than 4 kt. The test procedure was to hover at a fixed altitude out-of-ground effect with a selected flap setting, with and without AFC. Data were taken first with AFC off, and then it was switched on and finally off again before changing the amplitude. This procedure was repeated for a range of flap settings, rotor rpm, $C\mu$, and F^+. Video records of tufts on the flap trailing edge (Fig. 24) showed attachment when the AFC was turned on and separation when it was turned off.

The essential results are summarized in Figs. 26 and 27. The curves of the variation of the rotor power coefficient with the weight coefficient were constructed from data taken at different rpm settings for a given flap deflection. Figure 26 shows the results applicable to success criterion 2. The AFC-off case is for a flap deflection of 70° corresponding to the minimum download condition without AFC. The AFC-on case is shown for a flap deflection of 75°, corresponding to the minimum download with AFC engaged. The AFC-on curve is below and to the right of the baseline curve, indicating that, with AFC, more weight can be carried for a given power. The resulting download reduction is approximately 150 lb, or 9%, which met the goal for criterion 2.

Figure 27 shows the results applicable to criterion 1. Here, both curves are for a flap setting of 75°. At this angle, the flow over the flaps was fully separated without AFC. With AFC applied, the flow on the flap was reattached, as shown by the reduced power required to

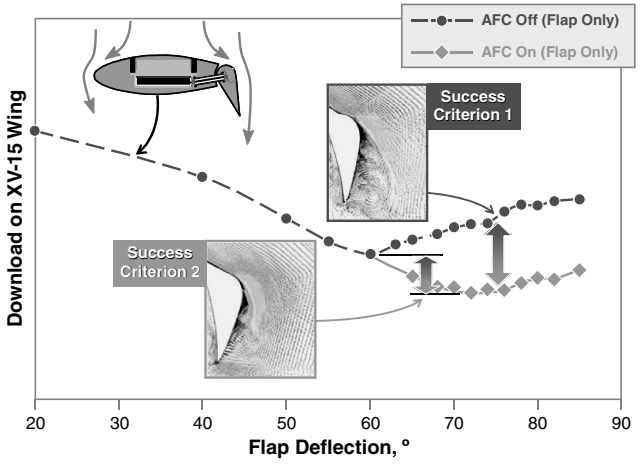

Fig. 25 Definition of flight-test success criteria.

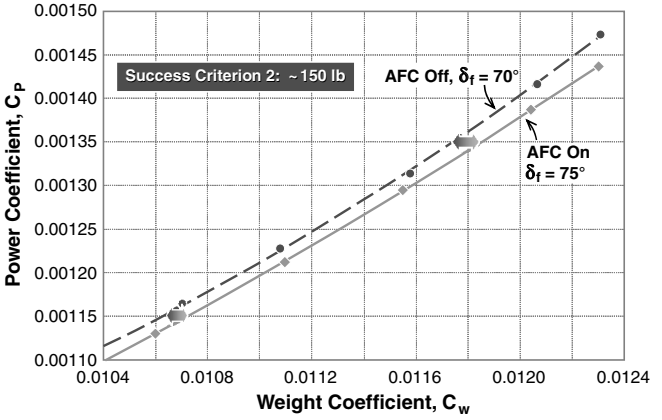

Fig. 26 XV-15 flight-test results; AFC performance for success criterion 2.

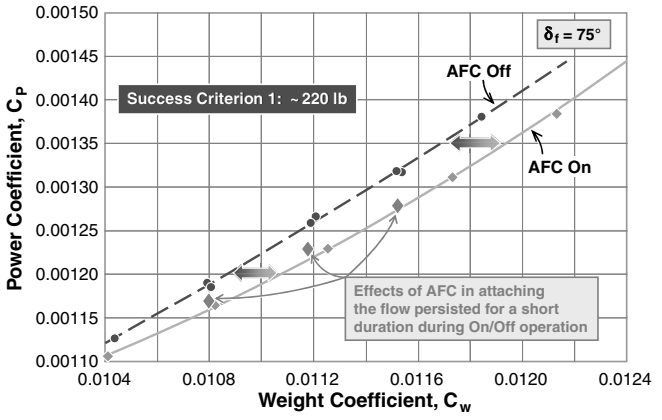

Fig. 27 XV-15 flight-test results; AFC performance for success criterion 1.

hover at the same weight and as confirmed by tuft observation. At high (constant) values of power coefficient, the reduction exceeded the 220 lb or 14% criterion, marked by the arrow in Fig. 27, which again met the goal.

In both the flight and model tests, the procedure was to measure the download with AFC off, then with it on, and again with it off. If the process was reversible, the off data would match. However, it was often noted during the flight tests that the effects of AFC lingered on after AFC was switched off, sometimes long enough to force the pilots to repeat the data or to descend slightly before taking the assigned third reading. It is known [12] that the $C\mu$ required to force reattachment of separated flow may be as much as an order of magnitude higher than the $C\mu$ needed to prevent separation. Consequently, environmental perturbations resulting from rotor-tip vortices striking the flap at blade passage frequencies may lock onto the AFC and provide sufficient amplitudes to keep the flow attached. Such coupling was observed during early V-22 powered-model tests, and it suggests a different procedure for the application of AFC. In this case, dynamic coupling between flap deflection and AFC amplitude during the initiation or transition to hover may prove more efficient. Such an arrangement requires sensors for closed-loop control and the use of algorithms that take advantage of this hysteresis.

VIII. Conclusions

AFC using zero-mass-flux periodic excitation successfully reduced the download on the wings of hovering tiltrotor aircraft. The effectiveness of AFC was demonstrated in a research program using scale models and a full-scale XV-15 tiltrotor aircraft. The following are the main results of this research program:

1) In 2-D wing/flap tests, the most effective location of the blowing slot was found to be near 10% flap chord.

2) In the 2-D tests with the 10% slot location, it was found that the greatest reduction in vertical drag (download) was achieved at $C\mu \sim 0.5\%$ and that larger values did not significantly reduce the download further.

3) In the 2-D tests, the best nondimensional AFC frequency was $F^+ < 1$.

4) On the powered XV-15 tiltrotor aircraft model, a passive Krueger flap was effective when AFC was applied to the trailing-edge flap. This was not found to be the case in the 2-D tests.

5) On the powered XV-15 model, with AFC applied to the trailing-edge flap and to the Krueger flap with the two 180° out of phase with each other, a reduction in download of 30% was achieved compared with the lowest value obtained without AFC.

6) Hover flight tests of the full-scale XV-15 aircraft showed that the download could be reduced by 9% (150 lb) by increasing the flap deflection from 70 to 75° and applying AFC to maintain attached flow on the flap.

7) Hover flight tests of the full-scale XV-15 aircraft showed that the flow on the flap was completely separated at a flap deflection of 75°. Activation of AFC reattached the flow, and it reduced the download at the same flap deflection by more than 14% at the higher power settings.

8) Tests on powered full-span scaled tiltrotor models can correctly reproduce full-scale download aerodynamics.

9) LES of the 2-D flow about the XV-15 wing section, with and without a Krueger flap, were useful in visualizing and interpreting the experimental results.

Acknowledgments

Three universities (University of Arizona, Tel Aviv University, and Illinois Institute of Technology) and two major aerospace companies (The Boeing Company and Bell Helicopter Textron, Inc.) were involved in this project, which was administered by the U.S. Army Research Office under contract number DAAD19-99-C-0023. Many people contributed to this program, which lasted over 4.5 years. The authors wish to acknowledge the assistance of J. McMichael, R. Wlezien, and S. Walker of the Defense Advanced Research Projects Agency, who steered this project to its successful conclusion. There were many technical contributors to this program whose names do not appear in the list of authors. Aerodynamic testing and computation were made by N. Anderberg, D. Cerchie, L. Cullen, A. Darabi, D. Greenblatt, R. Grife, A. Hassan, J. Kiedaisch, P. Kjellgren, M. Schmalzel, and A. Stalker. Special thanks are due to D. Hodder for his design of the hover rig and the rigorous calibration effort. The support of the Bell Helicopter Flight Test Team is greatly appreciated.

References

[1] McVeigh, M. A., "The V-22 Tilt Rotor Large-Scale Rotor Performance/Wing Download Test and Comparison with Theory," *11th European Rotorcraft Forum*, London, Sept. 1985.

[2] McCroskey, W., Spalart, P., Laub, G., and Maisel, M., "Airloads on Bluff Bodies, with Application to the Rotor Induced Downloads on Tilt-Rotor Aircraft," *Vertica*, Vol. 9, 1985, pp. 1–11.

[3] Maisel, M., Laub, G., and McCroskey, W. J., "Aerodynamic Characteristics of Two-Dimensional Wings at Angle of Attack Near 90 Degrees," NASA TM 88373, 1986.

[4] Felker, F., and Light, J., "Rotor/Wing Aerodynamic Interactions in Hover," *42nd American Helicopter Society Annual Forum*, Washington, D.C., American Helicopter Soc., Alexandria, VA, June 1986.

[5] Wood, T. L., and Peryea, M. A., "Reduction of Tiltrotor Download," *49th American Helicopter Society Annual Forum*, St. Louis, MO, American Helicopter Soc., Alexandria, VA, May 1993.

[6] Seifert, A., Bachar, T., Koss, D., Shepshelovich, M., and Wygnanski, I., "Oscillatory Blowing, a Tool to Delay Boundary Layer Separation," *AIAA Journal*, Vol. 31, No. 11, 1993, p. 2052. doi:10.2514/3.49121

[7] Nagib, H., Kiedaisch, J., Wygnanski, I., Stalker, A. D., Wood, T., and McVeigh, M. A., "First In-Flight Full-Scale Application of Active Flow Control: The XV-15 Tiltrotor Download Reduction," *NATO Specialists' Meeting*, Prague, NATO, 15 Sept. 2004.

[8] Kjellgren, P., Anderberg, N., and Wygnanski, "Download Alleviation by Periodic Excitation on a Typical Tiltrotor Configuration: Computation and Experiment," AIAA Flow 2000, Denver, CO, AIAA Paper 2000-2697, June 2000.

[9] Kjellgren, P., Cerchie, D., Cullen, L., and Wygnanski, I., "Active Flow Control on Bluff Bodies with Distinct Separation Locations," 1st AIAA Flow Control Conference, St. Louis, MO, AIAA Paper 2002-3069, June 2002.

[10] Kjellgren, P., Hassan, A., Sivasubramanian, J., Cullen, L., Cerchie, D., and Wygnanski, I., "Download Alleviation for the XV-15: Computations and Experiments for the Flow Around the Wing," AIAA Paper 2002-6007, 2002.

[11] Stalker, A., "The Effects of Krueger Flaps and Periodic Perturbations on the Download Alleviation of a Typical Tiltrotor Aircraft," M.S. Thesis, AME Department, Univ. of Arizona, Tucson, AZ, 2004.

[12] Nishri, B., and Wygnanski, I., "Effects of Periodic Excitation on Turbulent Flow Separation from a Flap," *AIAA Journal*, Vol. 36, No. 4, 1998, pp. 547–556. doi:10.2514/2.428